INTERNATIONAL JOURNAL OF
NUMERICAL ANALYSIS AND MODELING
Volume 16, Number 4, Pages 647–667

ORTHOGONAL SPLINE COLLOCATION FOR SINGULARLY PERTURBED REACTION DIFFUSION PROBLEMS IN ONE DIMENSION

PANKAJ MISHRA, KAPIL K. SHARMA, AMIYA K. PANI, AND GRAEME FAIRWEATHER

Abstract. An orthogonal spline collocation method (OSCM) with C^1 splines of degree $r \geq 3$ is analyzed for the numerical solution of singularly perturbed reaction diffusion problems in one dimension. The method is applied on a Shishkin mesh and quasi-optimal error estimates in weighted H^m norms for $m = 1, 2$ and in a discrete L^2-norm are derived. These estimates are valid uniformly with respect to the perturbation parameter. The results of numerical experiments are presented for C^1 cubic splines ($r = 3$) and C^1 quintic splines ($r = 5$) to demonstrate the efficacy of the OSCM and confirm our theoretical findings. Further, quasi-optimal *a priori* estimates in L^2, L^∞ and $W^{1,\infty}$-norms are observed in numerical computations. Finally, superconvergence of order $2r - 2$ at the mesh points is observed in the approximate solution and also in its first derivative when $r = 5$.

Key words. Singularly perturbed reaction diffusion problems, orthogonal spline collocation, Shishkin mesh, quasi-optimal global error estimates, superconvergence.

1. Introduction

In this paper, we consider singularly perturbed reaction diffusion problems of the form

$$Lu(x) := -\varepsilon u''(x) + a(x)u(x) = f(x), \quad x \in I \equiv (0, 1), \tag{1}$$

subject to the Dirichlet boundary conditions,

$$u(0) = 0, \quad u(1) = 0, \tag{2}$$

where the parameter ε is such that $0 < \varepsilon \ll 1$. It is assumed that the prescribed functions a and f are smooth on I with

$$a(x) \geq \alpha > 0, \quad x \in \overline{I}, \tag{3}$$

where α is a constant. Problems of this type are ubiquitous in the mathematical modeling of numerous real life phenomena; see, for example, [18, 21] and references therein. The solution of (1)–(2) exhibits a multi scale character. Specifically, there is a thin transition layer, often called a boundary layer, at one or both ends of the interval I, in which the solution varies rapidly, while away from the layer, the solution behaves smoothly and varies gradually. This singular behavior of the solution presents some challenges in the development of methods to solve this type of problem accurately and efficiently. One of the most successful approaches involves the use of layer-adapted meshes such as Shishkin meshes [24], which yield methods that converge uniformly, regardless of the magnitude of the parameter ε; see, for example, [17].

In the literature, much attention has been devoted to the development of numerical methods for the solution of singularly perturbed differential equations which converge uniformly with respect to the parameter ε. This work is chronicled in numerous texts, research papers, such as [2, 17, 15, 18, 20, 21, 22, 23, 25, 27] and

Received by the editors on November 7, 2017.
2000 *Mathematics Subject Classification.* 65L11, 65L60, 65L70.

survey articles [11, 12, 13]. Broadly speaking, there are three principal approaches to solving (1)–(2) numerically, namely; finite difference methods, finite element methods and spline collocation methods. Particular attention has been devoted to the latter class of methods, especially, spline collocation based on smoothest splines such as classical C^2 cubic splines; see, [9, 10]. Invariably, these methods yield approximations of suboptimal accuracy. For example, cubic spline collocation applied to (1)–(2) cannot be more than second order accurate, a fact proved in [3]. A collocation method of optimal accuracy that has been used to solve a variety of problems involving ordinary and partial differential equations is the orthogonal spline collocation method (OCSM); see, for example, [1]. The popularity of the orthogonal spline collocation approach is due to its conceptual simplicity, wide range of applicability and ease of implementation. This method, often called spline collocation at Gauss points in the literature, was originally formulated and analyzed over 40 years ago in the seminal paper [4], but has seen little use in the numerical solution of singularly perturbed problems.

In 1980, Flaherty and Mathon [8] used collocation methods with either piecewise polynomials or splines in tension to obtain accurate approximations of one dimensional singularly perturbed boundary value problems. In their paper, the authors state "*Unfortunately, collocation at the Gauss-Legendre points with piecewise polynomials is known to behave rather poorly on singularly-perturbed problems for any partition, where ε is much smaller than the minimum subinterval length.*" In an attempt to generalize the results of [4] to (1)-(2), the authors of [16] considered collocation methods with C^1-quadratic splines using a modified Shishkin mesh and derived almost second order convergence in the maximum norm. In their paper, the authors state, "*C^1-splines with arbitrary order for such problems presents an open task*". In the present article, we develop and analyze an OSCM with C^1 splines of order $r \geq 3$ for solving (1)-(2) using Shishkin meshes in weaker norms. In particular, we derive quasi-optimal estimates of order $(N^{-1}\log N)^{r+1-m}$ in weighted H^m-norms, $m = 1, 2$, and of order $(N^{-1}\log N)^{r+1}$ in a discrete L^2 norm, where N is the number of mesh subintervals. These estimates are valid uniformly with respect to the perturbation parameter ε. The results of numerical experiments confirm our theoretical findings. It is also observed from numerical experiments that error estimates in L^2, L^∞ and $W^{1,\infty}$-norms are quasi-optimal, which are uniform in ε. Moreover, they demonstrate the exceptional performance of the OSCM, especially its ability to yield high order approximations systematically. In [26], the OSCM with $r = 3$ on a Shishkin mesh is considered but, using a different analysis, it is proved that the convergence rate in $L^\infty(I)$ is $O(N^{-4}\log^5 N)$.

A brief outline of this paper is as follows. In Section 2, we introduce notation and some basic results used in the convergence analysis. In Section 3, the OSCM employing a Shishkin mesh is applied to discretize (1)–(2). Section 4 is devoted to the convergence analysis. In Section 5, the results of numerical experiments are presented which illustrate the efficacy of the method and confirm the analytical results. Moreover, they exhibit superconvergence properties of the method which, while anticipated, are as yet unproven. Concluding remarks are given in Section 6.

2. Preliminaries

2.1. Notation. Let $\pi_h = \{x_j\}_{j=0}^N$ denote a partition of $\overline{I} = [0, 1]$ with

$$0 = x_0 < x_1 < \ldots < x_{N-1} < x_N = 1.$$

Let

$$I_j = [x_{j-1}, x_j], \quad h_j = x_j - x_{j-1}, \quad j = 1, \ldots, N, \text{ and } h = \max_j h_j.$$

We define the finite dimensional subspace $\mathcal{M}_1^{r,0}$ of $H_0^1(I)$ by

$$\mathcal{M}_1^{r,0} = \{v_h \in C^1(I) : v_h|_{I_j} \in \mathcal{P}_r(I_j), \;\; j = 1, \ldots, N, \;\; v_h(0) = v_h(1) = 0\},$$

where $\mathcal{P}_r(I_j)$ denotes the set of all polynomials of degree $\leq r$ on I_j. Note that

$$\dim \mathcal{M}_1^{r,0} = N(r-1).$$

When $r = 3$, the space $\mathcal{M}_1^{3,0}$ is known as the space of piecewise Hermite cubics.

We now construct a Shishkin mesh, which is piecewise uniform.To this end, we divide the interval $[0, 1]$ into three subintervals, namely; $I_L = [0, \tau]$, $I_M = [\tau, 1-\tau]$ and $I_R = [1-\tau, 1]$, where the transition parameter τ is chosen such that

$$\tau = \min\left\{1/4, (r+1)(\varepsilon/\alpha)^{1/2} \log N\right\}, \tag{4}$$

where $N = 2^\ell$, $\ell \geq 3$, and α is given in (3). We divide each of the subintervals $[0, \tau]$ and $[\tau, 1-\tau]$ into $N/4$ equal subdivisions while the interval $[1-\tau, 1]$ is divided into $N/2$ equal subdivisions, so that

- on $[0, \tau]$, the mesh points are $x_i = x_{i-1} + h_{1,max}$, for $i = 1, 2, 3, ..., N/4$, with $h_{1,max} = 4\tau/N$;
- on $[\tau, \tau - 1]$, $x_i = x_{i-1} + h_{2,max}$, for $i = N/4 + 1, ..., 3N/4$, with $h_{2,max} = 2(1-2\tau)/N$;
- on $[1-\tau, 1]$, we have $x_i = x_{i-1} + h_{1,max}$, for $i = 3N/4 + 1, ..., N$, with $h_{1,max} = 4\tau/N$.

Let $\{\lambda_k\}_{k=1}^{r-1}$ and $\{\omega_k\}_{k=1}^{r-1}$ denote the nodes and weights, respectively, of the $(r-1)$-point Gauss-Legendre quadrature rule on I. Let

$$\mathcal{G} = \{\xi_p\}_{p=1}^{N(r-1)}$$

be the set of points in I, where

$$\xi_{(j-1)(r-1)+k} = x_{j-1} + h_j \lambda_k, \quad k = 1, 2, ...r-1, \quad j = 1, ..., N.$$

For any $\phi, \psi \in C^0(\bar{I})$, we define the discrete inner product

$$\langle \phi, \psi \rangle = \sum_{j=1}^{N} \langle \phi, \psi \rangle_j = \sum_{j=1}^{N} \sum_{k=1}^{r-1} \omega_{j,k} \phi(\xi_{j,k}) \psi(\xi_{j,k}),$$

with

$$\langle \phi, \phi \rangle_j = \sum_{k=1}^{r-1} \omega_{j,k} \phi(\xi_{j,k}) \psi(\xi_{j,k})$$

and its induced norm

$$|\phi|_j := \langle \phi, \phi \rangle_j^{1/2} = \left(\sum_{k=1}^{r-1} \omega_{j,k} \phi^2(\xi_{j,k}) \right)^{1/2}, \quad |\phi|_D = \left(\sum_{j=1}^{N} |\phi|_j^2 \right)^{1/2}.$$

In the following, we denote by C a positive constant which is independent of h and the parameter, ε.

2.2. Basic Lemmas. The first lemma is a fundamental property of Gauss-Legendre quadrature.

Lemma 2.1. *For $\phi \in \mathcal{P}_{2r-3}(I_j), 1 \le j \le N$,*

$$\int_{I_j} \phi(x)dx = \sum_{k=1}^{r-1} w_{j,k}\phi(\xi_{j,k}).$$

We recall the following results from [6].

Lemma 2.2. [6, Lemma 3.1] *For all $\phi, \psi \in \mathcal{M}_1^{r,0}$,*

$$-\langle \phi'', \psi\rangle = (\phi', \psi') - \phi'\psi|_0^1 + \left(1 - \frac{1}{r}\right)\int_0^1 B_r^{''}(x)^2 \sum_{j=1}^{N} \phi_j^{(r)}\psi_j^{(r)} h_j^{2r-1},$$

where $B_r''(x)$ is a multiple of the Legendre polynomial of degree $r-1$ on I.

Lemma 2.3. [6, Lemma 3.3] *If $\phi \in \mathcal{M}_1^{r,0}$, then*

$$\|\phi\|_{H_0^1}^2 \le -\langle \phi'', \phi\rangle \le \left(2 - \frac{1}{r}\right)\|\phi\|_{H_0^1}^2.$$

Lemma 2.4. [6, Eq. (3.4)] *If $\phi \in \mathcal{M}_1^{r,0}$, then*

$$|\phi|_D \le C\|\phi\|_{L^2(I)}. \tag{5}$$

Lemma 2.5. [6, Eq. (2.11)] *Suppose $u \in H^{r+3}(I_j)$, $j = 1, 2, \ldots, N$. Let $\eta = u - u_{\mathcal{H}}$, where $u_{\mathcal{H}}$ is the interpolant of u defined in* [6, pp. 8-9].[1] *Then*

$$|\eta^{(\ell)}|_j \le Ch_j^{r+1-\ell}\|u^{(r+1)}\|_{L^2(I_j)}, \quad \ell = 0, 1, \tag{6}$$

$$|\eta''|_j \le Ch_j^{r}\|u^{(r+2)}\|_{L^2(I_j)}, \tag{7}$$

$$|\langle \eta', 1\rangle_j| \le Ch_j^{r+3/2}\|u^{(r+2)}\|_{L^2(I_j)}, \tag{8}$$

$$|\langle \eta'', 1\rangle_j| \le Ch_j^{r+3/2}\|u^{(r+3)}\|_{L^2(I_j)}. \tag{9}$$

Lemma 2.6. *If $u \in H^{r+3}(I) \cap H_0^1(I)$, then*

$$\|\eta\|_{H^m} \le Ch^{r+1-m}\|u\|_{H^{r+1}}, \quad m = 0, 1, \tag{10}$$

and

$$\|\eta''\|_{L^2} \le Ch^{r-1}\|u\|_{H^{r+1}}. \tag{11}$$

Further,

$$\|\eta\|_{W^{m,\infty}(I)} \le Ch^{r+1-m}\|u\|_{W^{r+1,\infty}}, \quad m = 0, 1. \tag{12}$$

Proof. These results may be derived using the Peano Kernel Theorem. □

In the convergence analysis, we use the following regularity result for the solution u of (1)–(2).

Lemma 2.7. *For any positive integer s with $0 \le k \le s$, there exists a positive constant C independent of ε such that*

$$|u^{(k)}(x)| \le C\left[1 + \varepsilon^{-k/2}\left(e^{-x(\alpha/\varepsilon)^{1/2}} + e^{-(1-x)(\alpha/\varepsilon)^{1/2}}\right)\right], \quad x \in \overline{I}. \tag{13}$$

Proof. This result may be proved using the inductive argument in [18, pp. 39, Sect. 6, Lemma 1]. □

[1] When $r = 3$, $u_{\mathcal{H}}$ is the piecewise Hermite cubic interpolant of u.

3. The Orthogonal Spline Collocation Method

In the orthogonal spline collocation method, we seek $u_h \in \mathcal{M}_1^{r,0}$ satisfying

$$Lu_h(\xi) = f(\xi) \quad \text{for all } \xi \in \mathcal{G}. \tag{14}$$

The solution of (14) can be written in the form

$$u_h(x) = \sum_{j=1}^{N(r-1)} \alpha_j \mathcal{B}_j(x), \quad x \in \bar{I}, \tag{15}$$

where $\{\mathcal{B}_j\}_{j=1}^{N(r-1)}$ is the B-spline basis for $\mathcal{M}_1^{r,0}$. On substituting u_h in (14), we obtain the collocation equations

$$\sum_{j=1}^{N(r-1)} L\mathcal{B}_j(\xi)\alpha_j = f(\xi) \quad \text{for all } \xi \in \mathcal{G}, \tag{16}$$

which can be written as an almost block diagonal linear system of order $N(r-1)$ for the coefficients $\alpha_j, j = 1, \ldots, N(r-1)$. Such systems can be solved at cost of $O(N)$ using the package *COLROW* [5].

4. Convergence analysis

First note that (14) is equivalent to

$$\langle Lu_h, v_h \rangle = \langle f, v_h \rangle, \quad v_h \in \mathcal{M}_1^{r,0}, \tag{17}$$

which is used in the error analysis whereas (14) is used in computations.

In the analysis, it is convenient to use the following norm:

$$\|\phi\|_{1,\varepsilon} = \left(\varepsilon\|\phi'\|_{L^2}^2 + |a^{1/2}\phi|_D^2\right)^{1/2}. \tag{18}$$

Using the interpolant $u_{\mathcal{H}}$ of u given in [6, Pages 8-9], we write

$$u - u_h = (u - u_{\mathcal{H}}) - (u_h - u_{\mathcal{H}}) = \eta - \theta,$$

where $\eta = u - u_{\mathcal{H}}$ and $\theta = u_h - u_{\mathcal{H}}$.

Lemma 4.1. *Let $I = I_L \cup I_M \cup I_R$, where $I_L = (0, \tau)$, $I_M = (\tau, 1-\tau)$ and $I_R = (1-\tau, 1)$. If u is sufficiently smooth, then*

$$\begin{aligned} \|\theta\|_{1,\varepsilon} + |\theta|_D \le C \Big\{ & h_{1,max}^{r+1} \left(\|u^{(r+1)}\|_{L^2(I_L \cup I_R)} + \varepsilon^{1/2}\|u^{(r+2)}\|_{L^2(I_L \cup I_R)} \right. \\ & \left. + \varepsilon\|u^{(r+3)}\|_{L^2(I_L \cup I_R)} \right) + h_{2,max}^{r+1} \left(\|u^{(r+1)}\|_{L^2(I_M)} \right. \\ & \left. + \varepsilon^{1/2}\|u^{(r+2)}\|_{L^2(I_M)} + \varepsilon\|u^{(r+3)}\|_{L^2(I_M)} \right) \Big\}, \end{aligned} \tag{19}$$

and

$$\begin{aligned} \|\theta\|_{L^2(I)} + \|\theta'\|_{L^2(I)} \le C \Big\{ & h_{1,max}^{r+1} \left(\varepsilon^{-1/2}\|u^{(r+1)}\|_{L^2(I_L \cup I_R)} + \|u^{(r+2)}\|_{L^2(I_L \cup I_R)} \right. \\ & \left. + \varepsilon^{1/2}\|u^{(r+3)}\|_{L^2(I_L \cup I_R)} \right) + h_{2,max}^{r+1} \left(\varepsilon^{-1/2}\|u^{(r+1)}\|_{L^2(I_M)} \right. \\ & \left. + \|u^{(r+2)}\|_{L^2(I_M)} + \varepsilon^{1/2}\|u^{(r+3)}\|_{L^2(I_M)} \right) \Big\}. \end{aligned} \tag{20}$$

Proof. From (1) and (17), we obtain

$$\langle L(u - u_h), v_h \rangle = 0, \tag{21}$$

which we write as

$$\langle L\theta, v_h \rangle = \langle L\eta, v_h \rangle. \tag{22}$$

Since $\theta \in \mathcal{M}_1^{r,0}$, we obtain

$$\begin{aligned} \langle L\theta, \theta\rangle &= -\varepsilon \langle \eta'', \theta\rangle_j + \langle a\eta, \theta\rangle \\ &= -\varepsilon \sum_{j=1}^{N} \langle \eta'', \theta - \overline{\theta}\rangle - \varepsilon \sum_{j=1}^{N} \langle \eta'', 1\rangle \overline{\theta} + \left\langle a^{1/2}\eta, a^{1/2}\theta \right\rangle, \end{aligned} \tag{23}$$

where

$$\overline{\theta}_j := \overline{\theta}|_{I_j} = \frac{1}{h_j} \int_{I_j} \theta dx.$$

For the term on the left hand side of (23), we have

$$\langle L\theta, \theta\rangle = -\varepsilon \langle \theta'', \theta\rangle + |a^{1/2}\theta|_D^2 \geq \varepsilon \|\theta'\|_{L^2}^2 + |a^{1/2}\theta|_D^2 = \|\theta\|_{1,\varepsilon}^2, \tag{24}$$

using Lemma 2.3. For the first term on the right hand side of (23), a use of (7) yields

$$\begin{aligned} -\varepsilon \left\langle \eta'', \theta - \overline{\theta}\right\rangle &\leq \varepsilon |\eta''|_D \, |\theta - \overline{\theta}|_D \\ &\leq C\varepsilon \sum_{j=1}^{N} h_j^{r+1} \|u^{(r+2)}\|_{L^2(I_j)} \|\theta'\|_{L^2(I_j)} \\ &\leq C\varepsilon h^{r+1} \|u^{(r+2)}\|_{L^2} \|\theta'\|_{L^2} \\ &\leq C\varepsilon h^{2r+2} \|u^{(r+2)}\|_{L^2}^2 + \frac{1}{2}\varepsilon \|\theta'\|_{L^2}^2. \end{aligned} \tag{25}$$

For the second term on right hand side of (23), we use (9) to obtain

$$\begin{aligned} -\varepsilon \langle \eta'', 1\rangle \overline{\theta} &= \varepsilon \sum_{j=1}^{N} \langle \eta'', 1\rangle_j \overline{\theta}_j \\ &\leq C\varepsilon \sum_{j=1}^{N} h_j^{r+3/2} \|u^{(r+3)}\|_{L^2(I_j)} \, h_j^{-1} \langle \theta, 1\rangle_j \\ &\leq C\varepsilon \sum_{j=1}^{N} h_j^{r+1} \|u^{(r+3)}\|_{L^2(I_j)} \, |a^{1/2}\theta| \cdot \|a^{-1/2}\|_\infty \\ &\leq C\varepsilon h^{r+1} \|u^{(r+3)}\|_{L^2} \, |a^{1/2}\theta| \\ &\leq C\varepsilon^2 h^{2r+2} \|u^{(r+3)}\|_{L^2}^2 + \frac{1}{4}|a^{1/2}\theta|^2. \end{aligned} \tag{26}$$

Finally, for the third term on the right hand side of (23), we use (6) with $\ell = 0$ to obtain

$$\begin{aligned} \left\langle a^{1/2}\eta, a^{1/2}\theta \right\rangle &\leq |a^{1/2}\eta|_D \, |a^{1/2}\theta|_D \\ &\leq C \, |\eta|_D \, |a^{1/2}\theta|_D \\ &\leq Ch^{r+1} \|u^{(r+1)}\|_{L^2} \cdot |a^{1/2}\theta| \\ &\leq Ch^{2r+2} \|u^{(r+1)}\|_{L^2}^2 + \frac{1}{4}|a^{1/2}\theta|^2. \end{aligned} \tag{27}$$

On substituting (24)–(27) in (23), it follows that

$$\begin{aligned} \|\theta\|_{1,\varepsilon} \leq C \Big\{ & h_{1,max}^{r+1} \left(\|u^{(r+1)}\|_{L^2(I_L \cup I_R)} + \varepsilon^{1/2} \|u^{(r+2)}\|_{L^2(I_L \cup I_R)} + \varepsilon \|u^{(r+3)}\|_{L^2(I_L \cup I_R)} \right) \\ & + h_{2,max}^{r+1} \left(\|u^{(r+1)}\|_{L^2(I_M)} + \varepsilon^{1/2} \|u^{(r+2)}\|_{L^2(I_M)} + \varepsilon \|u^{(r+3)}\|_{L^2(I_M)} \right) \Big\}, \end{aligned} \tag{28}$$

proving (19).

Using the Poincaré inequality,

$$\|\theta\|_{L^2} \leq C\|\theta'\|_{L^2},$$

in (28), we obtain (20). This completes the proof. □

Remark 4.1. *Note that (28) yields a superconvergence result for* $\|\theta\|_{1,\varepsilon}$.

4.1. An *a priori* $H^1_\varepsilon(I)$ estimate.

Theorem 4.1. *Let* $u \in H^{r+3}(I) \cap H^1_0(I)$ *and* $u_h \in \mathcal{M}^{r,0}_1$ *be the solutions of (1)–(2) and (17), respectively. Then*

$$\|u - u_h\|_{H^1_\varepsilon(I)} \leq C(N^{-1}\log N)^r, \tag{29}$$

and

$$|u - u_h|_D \leq C(N^{-1}\log N)^{r+1}. \tag{30}$$

Proof. From (4), we consider the two cases, $\tau = \frac{1}{4}$ and $\tau < \frac{1}{4}$.

Case I. When $\tau = \frac{1}{4}$, the mesh is uniform with $h_{1,max} = h_{2,max} = 1/N$, and we obtain from (4)

$$\varepsilon^{-1/2} \leq 4(r+1)\alpha^{-1/2}\log N. \tag{31}$$

From Lemma 2.7,

(32)

$$\|u^{(r+1)}\|^2_{L^2} \leq C\left\{1 + \varepsilon^{-(r+1)}\int_0^1 \left(e^{-2x(\alpha/\varepsilon)^{1/2}} + e^{-2(1-x)(\alpha/\varepsilon)^{1/2}}\right)\, dx\right\} \leq C\varepsilon^{-(r+1)}.$$

Similarly,

$$\varepsilon\|u^{(r+2)}\|^2_{L^2} + \varepsilon^2\|u^{(r+3)}\|^2_{L^2} \leq C\left(\varepsilon + \varepsilon^2 + \varepsilon^{-(r+1)}\varepsilon^{1/2}\right) \leq C\varepsilon^{-(r+1)}. \tag{33}$$

Therefore, on substituting (31) − (33) in (19), we obtain

$$|\theta|^2_D + \varepsilon\|\theta'\|^2_{L^2(I)} \leq C\left(N^{-1}\log N\right)^{2(r+1)}. \tag{34}$$

Case II. Here,

$$\tau = (r+1)(\varepsilon/\alpha)^{1/2}\log N \text{ with } \tau < \frac{1}{4}, \tag{35}$$

and the mesh is piecewise uniform with mesh spacing $h_{1,max} = 4\tau/N$ in each of the subintervals I_L and I_R, and $h_{2,max} = 2(1-2\tau)/N$ in I_M. Therefore, from (35),

$$\varepsilon^{-1/2}h_{1,max} = \frac{4(r+1)\log N}{\alpha^{1/2}N}. \tag{36}$$

Using Lemma 2.7 and the fact that $\tau < \frac{1}{4}$, we obtain

$$\begin{aligned}\|u^{(r+1)}\|^2_{L^2(I_L\cup I_R)} &\leq C\left\{1 + \varepsilon^{-(r+1)}\int_{I_L\cup I_R}\left(e^{-2x(\alpha/\varepsilon)^{1/2}} + e^{-2(1-x)(\alpha/\varepsilon)^{1/2}}\right)\, dx\right\}\\ &\leq C\varepsilon^{-(r+1)}. \qquad (37)\end{aligned}$$

and for the remaining terms in (19), we have

$$\begin{aligned}\varepsilon\|u^{(r+2)}\|^2_{L^2(I_L\cup I_R)} + \varepsilon^2\|u^{(r+3)}\|^2_{L^2(I_L\cup I_R)} &\leq C\left(\varepsilon + \varepsilon^2 + \varepsilon^{-(r+1)}\right)\\ &\leq C\varepsilon^{-(r+1)}. \qquad (38)\end{aligned}$$

On combining (37) and (38) and using (36), we obtain

$$\begin{aligned} & Ch_{1,max}^{2(r+1)}\left(\|u^{(r+1)}\|^2_{L^2(I_L\cup I_R)}+\varepsilon\|u^{(r+2)}\|^2_{L^2(I_L\cup I_R)}+\varepsilon^2\|u^{(r+3)}\|^2_{L^2(I_L\cup I_R)}\right)\\ \leq & C\left(h_{1,max}^{2(r+1)}\varepsilon^{-(r+1)}\right)\\ \leq & C\left(N^{-1}\log N\right)^{2(r+1)}. \end{aligned} \tag{39}$$

In the subinterval I_M, the mesh is uniform with

$$h_{2,max}=\frac{2(1-2\tau)}{N} \quad \text{and} \quad \frac{1}{N}\leq h_{2,max}\leq\frac{2}{N}. \tag{40}$$

An application of Lemma 2.7 yields

$$\begin{aligned} \|u^{(r+1)}\|^2_{L^2(I_M)} =& C\int_\tau^{1-\tau}|u^{(r+1)}|^2\,dx\\ \leq & C\left\{1+\int_\tau^{1-\tau}\left(\varepsilon^{-(r+1)}e^{-2x(\alpha/\varepsilon)^{1/2}}+\varepsilon^{-(r+1)}e^{-2(1-x)(\alpha/\varepsilon)^{1/2}}\right)\,dx\right\}. \end{aligned} \tag{41}$$

Since

$$\lim_{\varepsilon\to 0}\varepsilon^{-m}e^{-\gamma/\sqrt{\varepsilon}}=0, \quad m,\gamma>0$$

it follows that

$$\varepsilon^{-m}e^{-\gamma/\sqrt{\varepsilon}}\leq C, \tag{42}$$

for small ε and $\gamma\neq 0$. Using (42) in (41) yields

$$\|u^{r+1}\|^2_{L^2(I_M)}\leq C. \tag{43}$$

Similarly, we obtain

$$\varepsilon\|u^{(r+2)}\|^2_{L^2(I_M)}+\varepsilon^2\|u^{(r+3)}\|^2_{L^2(I_M)} \quad \leq \quad C\varepsilon. \tag{44}$$

By combining (43) and (44), we obtain

$$h_{2,max}^{2(r+1)}\left(\|u^{r+1}\|^2_{L^2(I_M)}+\varepsilon\|u^{(r+2)}\|^2_{L^2(I_M)}+\varepsilon^2\|u^{(r+3)}\|^2_{L^2(I_M)}\right)\leq CN^{-2(r+1)}. \tag{45}$$

using (40). Finally, substituting (39) and (45) in (19) yields

$$|\theta|^2_D+\varepsilon\|\theta'\|^2_{L^2(I)}\leq C\left(N^{-1}\log N\right)^{2(r+1)}. \tag{46}$$

Since

$$\|u-u_h\|_{H^1_\varepsilon}\leq\|\eta\|_{1,\varepsilon}+\|\theta\|_{1,\varepsilon}, \tag{47}$$

and

$$|u-u_h|_D\leq\ |\eta|_D+|\theta|_D, \tag{48}$$

a use of (46)–(48), (6) with $\ell=0$, and (10) with $m=1$, completes the proof. □

Remark 4.2. *By extending the estimate in* [7, p. 21] *which is valid for* $r=3$*, we obtain*

$$\|\theta\|^2_{L^2(I_j)}\leq 4|\theta|^2_j+2h_j^2\varepsilon^{-1}\left(\varepsilon\|\theta'\|^2_{L^2(I_j)}\right). \tag{49}$$

Since

$$\|u-u_h\|_{L^2(I)}\leq\|\eta\|_{L^2(I)}+\|\theta\|_{L^2(I)}, \tag{50}$$

on using (49), (50) *and* (46) *with* (10) *with* $m=0$*, we obtain*

$$\|u-u_h\|_{L^2(I)}\leq C\left(1+\varepsilon^{-1/2}N^{-1}\right)(N^{-1}\log N)^{r+1}. \tag{51}$$

Remark 4.3. *Since $\theta \in H_0^1$, we have, on using the Sobolev inequality,*

$$\|\theta\|_{L^\infty(I)} \leq C\|\theta'\|_{L^2(I)}. \tag{52}$$

Then

$$\|u - u_h\|_{L^\infty(I)} \leq \|\eta\|_{L^\infty(I)} + \varepsilon^{-1/2}\varepsilon^{1/2}\|\theta\|_{L^\infty(I)}, \tag{53}$$

and using (12) *with* $m = 0$, (52) *and* (46), *we obtain*

$$\|u - u_h\|_{L^\infty(I)} \leq C\left\{(N^{-1}\log N)^{r+1} + \varepsilon^{-1/2}N^{-(r+2)}\right\}. \tag{54}$$

4.2. An *a priori* $H^2_\varepsilon(I)$ **estimate.** Here, we use the norm

$$\|v\|_{2,\varepsilon} = \left(\|v\|^2_{1,\varepsilon} + \varepsilon^2\|v''\|^2_{L^2}\right)^{1/2}.$$

Lemma 4.2. *If u is sufficiently smooth, then*

$$\begin{aligned}\|\theta\|^2_{2,\varepsilon(I)} \leq C\Big\{&h^{2r}_{1,max}\left(h^2_{1,max}\|u^{(r+1)}\|^2_{L^2(I_L\cup I_R)} + (\varepsilon^2 + h^2_{1,max}\varepsilon)\|u^{(r+2)}\|^2_{L^2(I_L\cup I_R)}\right.\\ &\left.+\varepsilon^2 h^2_{1,max}\|u^{(r+3)}\|^2_{L^2(I_L\cup I_R)}\right) + h^{2r}_{2,max}\left(h^2\|u^{(r+1)}\|^2_{L^2(I_M)}\right.\\ &\left.+(\varepsilon^2 + h^2_{2,max}\varepsilon)\|u^{(r+2)}\|^2_{L^2(I_M)} + \varepsilon^2 h^2_{2,max}\|u^{(r+3)}\|^2_{L^2(I_M)}\right)\Big\}.\end{aligned} \tag{55}$$

Proof. Choose $v_h = -\varepsilon\theta''$ in (22) to obtain

$$\begin{aligned}\langle L\theta, -\varepsilon\theta''\rangle = -\varepsilon\langle L\eta, \theta''\rangle =&\varepsilon^2\langle\eta'', \theta''\rangle - \varepsilon\langle a\eta, \theta''\rangle\\ \leq&\varepsilon^2\,|\eta''|_D\,|\theta''|_D + C\varepsilon\,|\eta|_D\,|\theta''|_D.\end{aligned} \tag{56}$$

For the term on the left hand side of (56), we note that

$$\langle L\theta, -\varepsilon\theta''\rangle_j = \varepsilon^2|\theta''|^2_j - \varepsilon\langle a\theta, \theta''\rangle_j. \tag{57}$$

Thus, on using (56) and (57),

$$\varepsilon^2|\theta''|^2_j \leq C\left(\varepsilon|\eta''|_j + |\eta|_j + |a^{1/2}\theta|_j\right)(\varepsilon|\theta''|_j). \tag{58}$$

Using (7), (6) with $\ell = 0$, and (19), we then obtain

$$\begin{aligned}\varepsilon|\theta''|_j &\leq C\left(\varepsilon|\eta''|_j + |\eta|_j + |a^{1/2}\theta|_j\right)\\ &\leq C\left(\varepsilon h_j^r\|u^{(r+2)}\|_{L^2(I_j)} + h_j^{r+1}\|u^{(r+1)}\|_{L^2(I_j)} + |a^{1/2}\theta|_j\right)\\ &\leq C\left(h_j^{r+1}\|u^{(r+1)}\|_{L^2(I_j)} + (\varepsilon + h_j\varepsilon^{1/2})h_j^r\|u^{(r+2)}\|_{L^2(I_j)}\right.\\ &\quad\left.+\varepsilon h_j^{r+1}\|u^{(r+3)}\|_{L^2(I_j)}\right).\end{aligned} \tag{59}$$

From Lemma 2.1,

$$|\theta''|_D = \|\theta''\|_{L^2}. \tag{60}$$

Thus, using (60) in (59),

$$\begin{aligned}\|\theta\|^2_{2,\varepsilon} &= \sum_{j=1}^N\left(\varepsilon^2\|\theta''\|^2_{L^2(I_j)} + \|\theta\|^2_{H^1_\varepsilon(I_j)}\right)\\ &\leq C\Big\{h^{2r}_{1,max}\left(h^2_{1,max}\|u^{(r+1)}\|^2_{L^2(I_L\cup I_R)} + (\varepsilon^2 + h^2_{1,max}\varepsilon)\|u^{(r+2)}\|^2_{L^2(I_L\cup I_R)}\right.\\ &\quad\left.+\varepsilon^2 h^2_{1,max}\|u^{(r+3)}\|^2_{L^2(I_L\cup I_R)}\right) + h^{2r}_{2,max}\left(h^2_{2,max}\|u^{(r+1)}\|^2_{L^2(I_M)}\right.\\ &\quad\left.+(\varepsilon^2 + h^2_{2,max}\varepsilon)\|u^{(r+2)}\|^2_{L^2(I_M)} + \varepsilon^2 h^2_{2,max}\|u^{(r+3)}\|^2_{L^2(I_M)}\right)\Big\}\end{aligned} \tag{61}$$

as desired. This concludes the proof. □

Theorem 4.2. *Let $u \in H^{r+3}(I) \cap H_0^1(I)$ and $u_h \in \mathcal{M}_1^{r,0}$ be the solutions of (1)–(2) and (17), respectively. Then,*

$$\|u - u_h\|_{2,\varepsilon} \leq C(N^{-1}\log N)^{r-1}.$$

Proof. As before, we consider the two cases, $\tau = 1/4$ and $\tau < 1/4$.
Case I. When $\tau = 1/4$, the mesh is uniform with $h_{1,max} = h_{2,max} = 1/N$ and (31) holds. From Lemma 2.7,

$$\begin{aligned} h_{1,max}^2\|u^{r+1}\|_{L^2(I)}^2 &\leq Ch_{1,max}^2\left\{1 + \varepsilon^{-(r+1)}\int_0^1 \left(e^{-2x(\alpha/\varepsilon)^{1/2}} + e^{-2(1-x)(\alpha/\varepsilon)^{1/2}}\right)\, dx\right\} \\ &\leq C\left(h_{1,max}^2 + h_{1,max}^2\varepsilon^{-1}\varepsilon^{-r}\right). \end{aligned} \tag{62}$$

Similarly,

$$\begin{aligned} (\varepsilon^2 + h_{1,max}^2\varepsilon)\|u^{r+2}\|_{L^2(I)}^2 + \varepsilon^2 h_{1,max}^2\|u^{r+2}\|_{L^2(I)}^2 &\leq C\left(\varepsilon^{-r} + \varepsilon^2 h_{1,max}^2 + h^2\varepsilon^{-1}\varepsilon^{-r}\right) \\ &\leq C\left(\varepsilon^{-r} + h_{1,max}^2\varepsilon^{-1}\varepsilon^{-r}\right). \end{aligned} \tag{63}$$

Substituting (31) and (63) in (55), we obtain

$$\begin{aligned} \|\theta\|_{2,\varepsilon(I)}^2 &\leq Ch^{2r}\left(h^2 + \varepsilon^{-r} + h^2\varepsilon^{-1}\varepsilon^{-r}\right) \\ &\leq CN^{-2r}\left(N^{-2} + (\log N)^{2r} + \left(\frac{\log N}{N}\right)^2(\log N)^{2r}\right) \\ &\leq \left(N^{-1}\log N\right)^{2r}. \end{aligned} \tag{64}$$

Case II. Here,

$$\tau = (r+1)(\varepsilon/\alpha)^{1/2}\log N \text{ with } \tau < 1/4,$$

and the mesh is piecewise uniform with mesh spacing $h_{1,max} = 4\tau/N$ in I_L and I_R and $h_{2,max} = 2(1-2\tau)/N$ in I_M, and (40) holds. From Lemma 2.7,

$$\begin{aligned} &h_{1,max}^2\|u^{r+1}\|_{L^2(I_L\cup I_R)}^2 \\ \leq& Ch_{1,max}^2\left\{1 + \varepsilon^{-(r+1)}\int_{I_L\cup I_R}\left(e^{-2x(\alpha\varepsilon)^{1/2}} + e^{-2(1-x)(\frac{\alpha}{\varepsilon})^{1/2}}\right)\, dx\right\} \\ \leq& Ch_{1,max}^2\left(1 + \varepsilon^{-(r+1)}\right). \end{aligned} \tag{65}$$

Similarly, for other terms

$$\begin{aligned} &(\varepsilon^2 + h_{1,max}^2\varepsilon)\|u^{r+2}\|_{L^2(I_L\cup I_R)}^2 + \varepsilon^2 h_{1,max}^2\|u^{r+2}\|_{L^2(I_L\cup I_R)}^2 \\ \leq& C\left(\varepsilon^{-r} + \varepsilon^2 h_{1,max}^2 + h_{1,max}^2\varepsilon^{-1}\varepsilon^{-r}\right) \\ \leq& C\left(\varepsilon^{-r} + h_{1,max}^2\varepsilon^{-1}\varepsilon^{-r}\right). \end{aligned} \tag{66}$$

By combining (65) and (66), we obtain

$$\begin{aligned} &h_{1,max}^{2r}\left(h_{1,max}^2\|u^{r+1}\|_{L^2(I_L\cup I_R)}^2 + (\varepsilon^2 + h_{1,max}^2\varepsilon)\|u^{r+2}\|_{L^2(I_L\cup I_R)}^2\right. \\ &\left.+\varepsilon^2 h_{1,max}^2\|u^{r+2}\|_{L^2(I_L\cup I_R)}^2\right) \\ \leq& C\, h_{1,max}^{2r}\left\{h_{1,max}^2\left(1 + \varepsilon^{-(r+1)}\right) + \varepsilon^{-r}\right\}. \end{aligned} \tag{67}$$

Substituting (40) in (67),

$$\begin{aligned} & h_{1,max}^{2r}\left(h_{1,max}^2\|u^{r+1}\|_{L^2(I_L\cup I_R)}^2+(\varepsilon^2+h_{1,max}^2\varepsilon)\|u^{r+2}\|_{L^2(I_L\cup I_R)}^2\right.\\ & \left.+\varepsilon^2h_{1,max}^2\|u^{r+2}\|_{L^2(I_L\cup I_R)}^2\right)\\ \leq & C\left\{N^{-2(r+1)}+N^{-2r}(\log N)^{2r}\right\}. \end{aligned} \tag{68}$$

In the subinterval I_M, the mesh is uniform as in (40). Hence, an application of Lemma 2.7 and the use of (42) leads to

$$\begin{aligned} & h_{2,max}^2\|u^{r+1}\|_{L^2(I_M)}^2\\ \leq & Ch_{2,max}^2\left\{1+\int_\tau^{1-\tau}\left(\varepsilon^{-(r+1)}e^{-2x(\frac{\alpha}{\varepsilon})^{1/2}}+\varepsilon^{-(r+1)}e^{-2(1-x)(\frac{\alpha}{\varepsilon})^{1/2}}\right)\,dx\right\}\\ \leq & CN^{-2}. \end{aligned} \tag{69}$$

Similarly,

$$(\varepsilon^2+h_{2,max}^2\varepsilon)\|u^{r+2}\|_{L^2(I_M)}^2+\varepsilon^2h_{2,max}^2\|u^{r+2}\|_{L^2(I_M)}^2\leq C\left(\varepsilon^2+h_{2,max}^2\varepsilon+h^2\varepsilon^2\right). \tag{70}$$

Combining (69) and (70) gives

$$\begin{aligned} & h_{2,max}^{2r}\left(h_{2,max}^2\|u^{r+1}\|_{L^2(I_M)}^2+(\varepsilon^2+h_{2,max}^2\varepsilon)\|u^{r+2}\|_{L^2(I_M)}^2\right.\\ & \left.+\varepsilon^2h_{2,max}^2\|u^{r+2}\|_{L^2(I_M)}^2\right)\\ \leq & C\left(N^{-2}+\varepsilon^2+\varepsilon N^{-2}\right)N^{-2r}. \end{aligned} \tag{71}$$

On substituting (68) and (71) in (55) with (64), we have

$$\begin{aligned} \|\theta\|_{2,\varepsilon}^2 & \leq C\left(\varepsilon^{1/2}\log N\left(N^{-2(r+1)}+\left(N^{-1}\log N\right)^{2r}\right)+\left(N^{-2}+\varepsilon^2+\varepsilon N^{-2}\right)N^{-2r}\right)\\ & \leq C\left(N^{-1}\log N\right)^{2r}. \end{aligned} \tag{72}$$

Thus, from (72) and (11),

$$\|u-u_h\|_{2,\varepsilon}\leq\|\eta\|_{2,\varepsilon}+\|\theta\|_{2,\varepsilon}\leq C\left(N^{-1}\log N\right)^{r-1},$$

as desired. □

Remark 4.4. *For $\varepsilon\ll 1$,*

$$\|\theta\|_{H^2}^2=\|\theta''\|_{L^2}^2+\|\theta'\|_{L^2}^2+\|\theta\|_{L^2}^2=\varepsilon^{-2}\left(\varepsilon^2\|\theta''\|_{L^2}^2+\varepsilon^2\|\theta'\|_{L^2}^2+\varepsilon^2\|\theta\|_{L^2}^2\right)\leq\varepsilon^{-2}\|\theta\|_{2,\varepsilon}^2,$$

and using (61).

$$\begin{aligned} \|\theta\|_{H^2}^2 \leq C\Big\{ & h_{1,max}^{2r}\left(\varepsilon^{-2}h_{1,max}^2\|u^{(r+1)}\|_{L^2(I_L\cup I_R)}^2+(1+h_{1,max}^2\varepsilon^{-1})\|u^{(r+2)}\|_{L^2(I_L\cup I_R)}^2\right.\\ & \left.+h_{1,max}^2\|u^{(r+3)}\|_{L^2(I_L\cup I_R)}^2\right)+h_{2,max}^{2r}\left(\varepsilon^{-2}h_{2,max}^2\|u^{(r+1)}\|_{L^2(I_M)}^2\right.\\ & \left.+(1+h_{2,max}^2\varepsilon^{-1})\|u^{(r+2)}\|_{L^2(I_M)}^2+h_{2,max}^2\|u^{(r+3)}\|_{L^2(I_M)}^2\right)\Big\}. \end{aligned}$$

Since

$$\|\theta\|_{W^{1,\infty}}\leq C\|\theta\|_{H^2}, \tag{73}$$

we obtain

$$\begin{aligned} \|u-u_h\|_{W_\infty^1} & \leq \|\eta\|_{W_\infty^1}+\varepsilon^{-1}\varepsilon\|\theta\|_{W_\infty^1},\\ & \leq C\left\{(N^{-1}\log N)^r\log N+\varepsilon^{-1}N^{-(r+1)}\right\}, \end{aligned} \tag{74}$$

on using (12) *with* $m = 1$, (73) *and* (72)

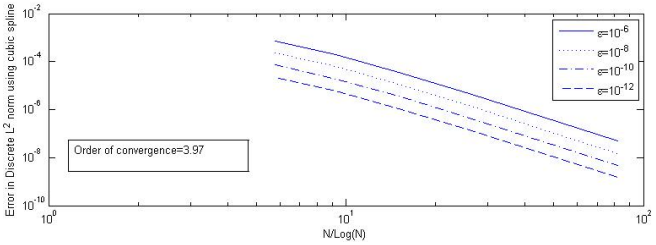

FIGURE 1. Discrete L^2 norm convergence using C^1 cubic splines.

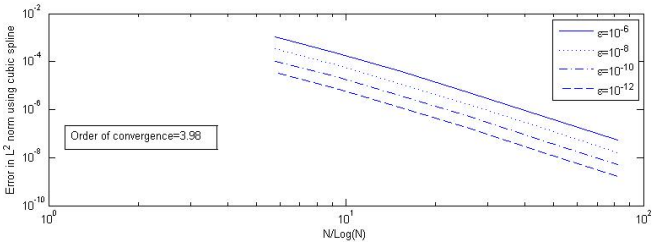

FIGURE 2. L^2 norm convergence using C^1 cubic splines

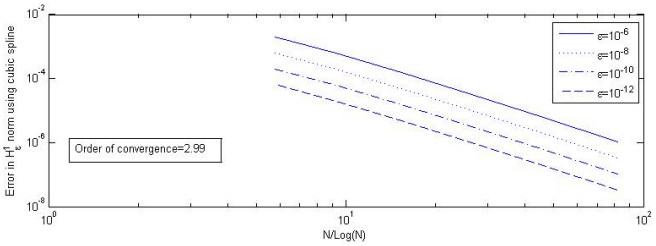

FIGURE 3. H^1_ε norm convergence using C^1 cubic splines

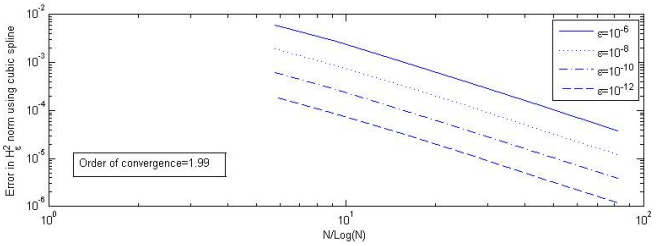

FIGURE 4. H^2_ε norm convergence using C^1 cubic splines

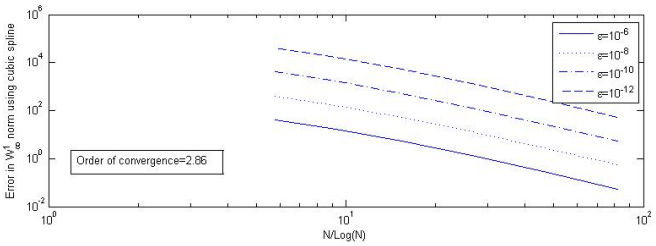

FIGURE 5. W^1_∞ norm convergence using C^1 cubic splines

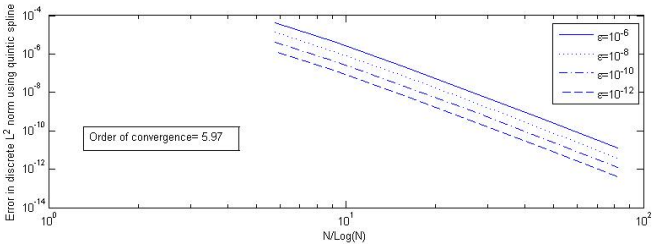

FIGURE 6. Discrete L^2 norm convergence using C^1 quintic splines

5. Numerical Example

In this section, we consider the following test problem from [14]:

$$-\varepsilon u''(x) + a(x)u(x) = f(x), \quad x \in (0,1), \qquad u(0) = u(1) = 0, \tag{75}$$

where $a(x) = 1 + x(1-x)$ and

$$\begin{aligned} f(x) &= 1 + x(1-x) + [2\varepsilon^{1/2} - x^2(1-x)]\exp[-(1-x)/\varepsilon^{1/2}] \\ &\quad + [2\varepsilon^{1/2} - x(1-x)^2]\exp(-x/\varepsilon^{1/2}). \end{aligned}$$

The exact solution of (75) is

$$u(x) = 1 + (x-1)\exp(-x/\varepsilon^{1/2}) - x\exp\left(-(1-x)/\varepsilon^{1/2}\right),$$

which has a boundary layer of width $\delta = O(\varepsilon^{1/2})$ at each end of $[0,1]$.

We present numerical results obtained by the OSCM with C^1 cubic ($r = 3$) and C^1 quintic ($r = 5$) splines. For each choice of subspace, error estimates in the $L^2, L^\infty, H^1_\varepsilon, H^2_\varepsilon$, $W^{1,\infty}$ and discrete norms for various values of ε and N are given. The L^∞ and $W^{1,\infty}$ errors were estimated by determining the maximum absolute error in the solution and its first derivative at 10 equally spaced points in each subinterval I_j, $j = 1, \ldots, N$. To estimate the L^2, H^1_ε and H^2_ε errors, three-point and five-point Gauss quadrature were used in the cubic and quintic cases, respectively. In each case, the experimental convergence rate of the error, for each fixed ε, was computed using

$$Rate = \frac{\log(E_N/E_{2N})}{\log(2\log N/\log(2N))},$$

where E_N denotes the norm of the error using N subintervals.

Results are given for C^1 cubic splines in Tables 1–6, and for the quintic case in Tables 7–12. In each case, the parameter uniform convergence of the method is obtained at the proven rate. Specifically, the results in Tables 4 and 10 and Tables

5 and 11 confirm the estimates given in Theorems 4.1 and 4.2, respectively. Tables 2 and 8 validate the optimal result obtained in discrete norms. However, in Tables 1 and 7 and Tables 3 and 9 confirm the results (51) and (54) respectively, while Tables 6 and 12 confirm the estimate given in (74).

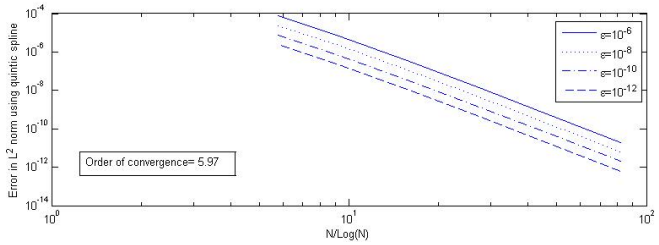

FIGURE 7. L^2 norm convergence using C^1 quintic splines

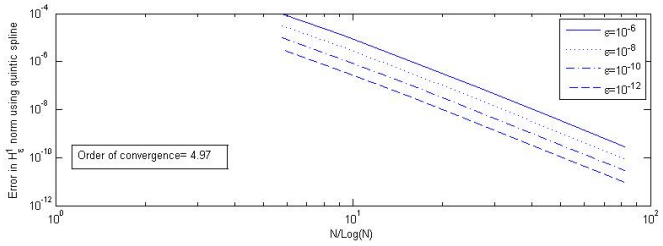

FIGURE 8. H^1_ε norm convergence using C^1 quintic splines

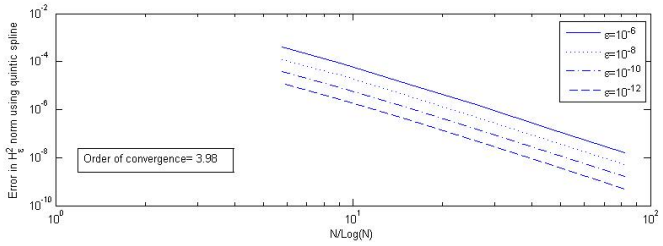

FIGURE 9. H^2_ε norm convergence using C^1 quintic splines

In many methods based on orthogonal spline collocation, superconvergence of order $2r-2$ in the approximate solution and its first derivative at the nodes is observed. For the cubic case, $r=3$, the results in Table 13 exhibit superconvergence in the approximate solution (for $r>3$) and its first derivative of order four, whereas the results in Tables 14 and 15 for quintics, $r=5$, demonstrate the anticipated eighth order accuracy in the approximate solution and its first derivative at the nodes.

We also include plots of the error in the various norms $(|.|_D,\ L^2, H^1_\varepsilon, H^2_\varepsilon, W^1_\infty)$ versus $N/\ln(N)$ on a log-log scale. The plots in Fig. 1–12 for cubic and quintic splines demonstrate the robustness of the method with respect to the parameter ε.

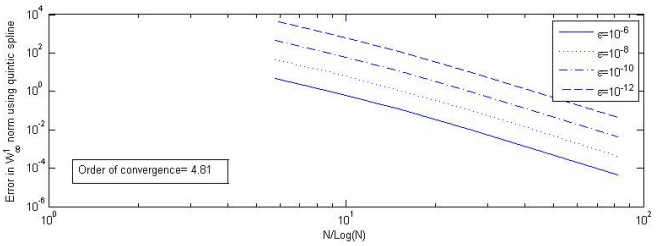

FIGURE 10. W^1_∞ norm convergence using C^1 quintic splines

In [14], the authors presented a parameter uniform method of order $O(N^{-1}\log N)^2$ in the maximum absolute nodal error only using cubic B-splines, and compared their results with some existing methods in the literature. When compared with the results in Table 4 of [14], the results presented in Table 16 of the present paper show that, as expected, the OSCM is substantially more accurate.

In [19], we present the results of numerical experiments which not only support the analytical results derived in the present paper, but also exhibit quasi-optimal estimates in other norms for Dirichlet problems as well as for problems with more general boundary conditions.

TABLE 1. L^2 error and convergence rate using C^1 cubic splines.

$N \rightarrow$ $\varepsilon \downarrow$	2^4	$2^5/Rate$	$2^6/Rate$	$2^7/Rate$	$2^8/Rate$	$2^9/Rate$
10^{-4}	3.4063e-03	7.7479e-04 3.150611	1.2268e-04 3.607947	1.5413e-05 3.848577	1.6924e-06 3.947446	1.7111e-07 3.982837
10^{-6}	1.0534e-03	2.3835e-04 3.161653	3.7637e-05 3.613295	4.7232e-06 3.850671	5.1842e-07 3.948175	5.2409e-08 3.983076
10^{-8}	3.3253e-04	7.5165e-05 3.163890	1.1865e-05 3.613888	1.4889e-06 3.850892	1.6341e-07 3.948250	1.6519e-08 3.983099
10^{-10}	1.0570e-04	2.3769e-05 3.175050	3.7511e-06 3.614366	4.7067e-07 3.850955	5.1658e-08 3.948268	5.2222e-09 3.983073
10^{-12}	3.5187e-05	7.5344e-06 3.279114	1.1865e-06 3.618596	1.4884e-07 3.851378	1.6335e-08 3.948370	1.6516e-09 3.982803

TABLE 2. Discrete-norm error and convergence rate using C^1 cubic splines.

$N \rightarrow$ $\varepsilon \downarrow$	2^4	$2^5/Rate$	$2^6/Rate$	$2^7/Rate$	$2^8/Rate$	$2^9/Rate$
10^{-4}	2.2901e-03	6.2019e-04 2.779437	1.0657e-04 3.447776	1.3835e-05 3.787841	1.5371e-06 3.926461	1.5602e-07 3.975993
10^{-6}	7.1082e-04	1.9096e-04 2.796434	3.2688e-05 3.455348	4.2368e-06 3.790717	4.7046e-07 3.927451	4.7745e-08 3.976315
10^{-8}	2.2436e-04	6.0225e-05 2.798184	1.0305e-05 3.456127	1.3354e-06 3.791013	1.4828e-07 3.927553	1.5048e-08 3.976348
10^{-10}	7.0934e-05	1.9040e-05 2.798360	3.2576e-06 3.456205	4.2216e-07 3.791043	4.6874e-08 3.927564	4.7570e-09 3.976352
10^{-12}	2.2431e-05	6.0207e-06 2.798377	1.0301e-06 3.456213	1.3350e-07 3.791046	1.4822e-08 3.927565	1.5042e-09 3.976352

TABLE 3. L^∞ error and convergence rate using C^1 cubic splines.

$N \to$ $\varepsilon \downarrow$	2^4	$2^5/Rate$	$2^6/Rate$	$2^7/Rate$	$2^8/Rate$	$2^9/Rate$
10^{-4}	2.81E-02	8.07E-03 2.65529	1.59E-03 3.180792	2.37E-04 3.532167	2.92E-05 3.738579	3.18E-06 3.854942
10^{-6}	2.75E-02	7.85E-03 2.666953	1.54E-03 3.187621	2.29E-04 3.535747	2.83E-05 3.740425	3.07E-06 3.85591
10^{-8}	2.74E-02	7.83E-03 2.668155	1.54E-03 3.188325	2.28E-04 3.536116	2.82E-05 3.740616	3.06E-06 3.85601
10^{-10}	2.74E-02	7.83E-03 2.668276	1.54E-03 3.188396	2.28E-04 3.536153	2.82E-05 3.740635	3.06E-06 3.85602
10^{-12}	2.74E-02	7.83E-03 2.668288	1.54E-03 3.188403	2.28E-04 3.536156	2.82E-05 3.740638	3.06E-06 3.855677

TABLE 4. H^1_ε error and convergence rate using C^1 cubic splines.

$N \to$ $\varepsilon \downarrow$	2^4	$2^5/Rate$	$2^6/Rate$	$2^7/Rate$	$2^8/Rate$	$2^9/Rate$
10^{-4}	6.5124e-03	2.0208e-03 2.489769	4.9165e-04 2.767079	1.0241e-04 2.910530	1.9443e-05 2.969019	3.4806e-06 2.989891
10^{-6}	2.0118e-03	6.2175e-04 2.498429	1.5094e-04 2.771260	3.1414e-05 2.912153	5.9622e-06 2.969580	1.0672e-06 2.990074
10^{-8}	6.3479e-04	1.9607e-04 2.499628	4.7589e-05 2.771696	9.9033e-06 2.912320	1.8795e-06 2.969638	3.3643e-07 2.990093
10^{-10}	2.0099e-04	6.1987e-05 2.502827	1.5044e-05 2.771806	3.1307e-06 2.912340	5.9417e-07 2.969644	1.0635e-07 2.990095
10^{-12}	6.4501e-05	1.9608e-05 2.533425	4.7574e-06 2.772479	9.9000e-07 2.912371	1.8789e-07 2.969647	3.3631e-08 2.990095

TABLE 5. H^2_ε error and convergence rate using C^1 cubic splines.

$N \to$ $\varepsilon \downarrow$	2^4	$2^5/Rate$	$2^6/Rate$	$2^7/Rate$	$2^8/Rate$	$2^9/Rate$
10^{-4}	1.9951e-02	8.8979e-03 1.718004	3.4218e-03 1.870814	1.1964e-03 1.949707	3.9450e-04 1.982444	1.2524e-04 1.994253
10^{-6}	6.1450e-03	2.7341e-03 1.723091	1.0500e-03 1.873367	3.6691e-04 1.950749	1.2097e-04 1.982815	3.8399e-05 1.994375
10^{-8}	1.9381e-03	8.6206e-04 1.723649	3.3104e-04 1.873630	1.1567e-04 1.950856	3.8133e-05 1.982853	1.2105e-05 1.994388
10^{-10}	6.1281e-04	2.7253e-04 1.724040	1.0465e-04 1.873660	3.6566e-05 1.950867	1.2055e-05 1.982857	3.8266e-06 1.994389
10^{-12}	1.9409e-04	8.6180e-05 1.727423	3.3093e-05 1.873699	1.1563e-05 1.950869	3.8120e-06 1.982857	1.2100e-06 1.994389

TABLE 6. $W^{1,\infty}$ error and convergence rate using C^1 cubic splines.

$N \to$ $\varepsilon \downarrow$	2^4	$2^5/Rate$	$2^6/Rate$	$2^7/Rate$	$2^8/Rate$	$2^9/Rate$
10^{-4}	4.1472e+00	1.7328e+00 1.856754	5.4185e-01 2.275736	1.3527e-01 2.574690	2.8894e-02 2.758320	5.5591e-03 2.864629
10^{-6}	4.0494e+01	1.6847e+01 1.865911	5.2522e+00 2.281645	1.3088e+00 2.578012	2.7929e-01 2.760117	5.3704e-02 2.865601
10^{-8}	4.0396e+02	1.6799e+02 1.866855	5.2355e+01 2.282255	1.3044e+01 2.578355	2.7832e+00 2.760303	5.3515e-01 2.865701
10^{-10}	4.0386e+03	1.6794e+03 1.866950	5.2338e+02 2.282316	1.3040e+02 2.578390	2.7823e+01 2.760322	5.3496e+00 2.865710
10^{-12}	4.0385e+04	1.6793e+04 1.866960	5.2337e+03 2.282322	1.3039e+03 2.578393	2.7822e+02 2.760324	5.3494e+01 2.865713

6. Concluding Remarks

We have presented an OSCM of arbitrary order on Shishkin meshes. Also, none of the problems stated in [8] were encountered. Quasi-optimal error estimates in various norms which are uniform with respect to the parameter ε are established and these estimates are supported by numerical experiments.

An OSCM for the convection–diffusion equation

$$Lu(x) := -\varepsilon u''(x) + a(x)u'(x) = f(x), \quad x \in I = (0,1),$$

TABLE 7. L^2 error and convergence rate using C^1 quintic splines.

$N \rightarrow$ $\varepsilon \downarrow$	2^4	$2^5/Rate$	$2^6/Rate$	$2^7/Rate$	$2^8/Rate$	$2^9/Rate$
10^{-4}	2.47E-04	2.26E-05 5.091993	1.33E-06 5.553161	3.92E-08 6.530152	6.36E-10 7.366523	1.00E-11 7.212013
10^{-6}	7.54E-05	6.85E-06 5.102251	4.00E-07 5.559053	1.74E-08 5.818563	6.28E-10 5.934806	2.01E-11 5.978414
10^{-8}	2.37E-05	2.16E-06 5.103327	1.26E-07 5.559671	5.47E-09 5.818846	1.98E-10 5.934915	6.34E-12 5.978355
10^{-10}	7.50E-06	6.82E-07 5.103475	3.98E-08 5.559734	1.73E-09 5.818874	6.25E-11 5.934893	2.00E-12 5.977808
10^{-12}	2.37E-06	2.16E-07 5.103889	1.26E-08 5.559752	5.47E-10 5.818892	1.98E-11 5.933981	6.33E-13 5.979354

TABLE 8. Discrete-norm error and convergence rate using C^1 quintic splines.

$N \rightarrow$ $\varepsilon \downarrow$	2^4	$2^5/Rate$	$2^6/Rate$	$2^7/Rate$	$2^8/Rate$	$2^9/Rate$
10^{-4}	1.3761e-04	1.3085e-05 5.006290	7.9060e-07 5.493890	1.4389e-08 7.432948	2.3420e-10 7.358654	3.6986e-12 7.209745
10^{-6}	4.1924e-05	3.9657e-06 5.017364	2.3889e-07 5.499808	1.0625e-08 5.775072	3.8811e-10 5.914272	1.2501e-11 5.970895
10^{-8}	1.3207e-05	1.2486e-06 5.018522	7.5191e-08 5.500428	3.3439e-09 5.775379	1.2213e-10 5.914394	3.9339e-12 5.970937
10^{-10}	4.1749e-06	3.9468e-07 5.018638	2.3766e-08 5.500490	1.0569e-09 5.775410	3.8602e-11 5.914406	1.2434e-12 5.970942
10^{-12}	1.3202e-06	1.2480e-07 5.018650	7.5152e-09 5.500497	3.3421e-10 5.775413	1.2206e-11 5.914407	3.9318e-13 5.970942

TABLE 9. L^∞ error and convergence rate using C^1 quintic splines.

$N \rightarrow$ $\varepsilon \downarrow$	$2^4/Rate$	$2^5/Rate$	$2^6/Rate$	$2^7/Rate$	$2^8/Rate$	$2^9/Rate$
10^{-4}	2.23E-03	2.48E-04 4.671359	1.97E-05 4.954352	4.67E-07 6.94743	8.90E-09 7.075665	1.53E-10 7.057549
10^{-6}	2.14E-03	2.38E-04 4.675659	1.89E-05 4.963024	1.04E-06 5.380193	4.40E-08 5.645782	1.56E-09 5.801667
10^{-8}	2.13E-03	2.37E-04 4.676107	1.88E-05 4.963932	1.03E-06 5.380735	4.38E-08 5.646091	1.56E-09 5.801841
10^{-10}	2.13E-03	2.37E-04 4.676152	1.88E-05 4.964023	1.03E-06 5.380789	4.38E-08 5.646122	1.55E-09 5.801858
10^{-12}	2.13E-03	2.37E-04 4.676157	1.88E-05 4.964032	1.03E-06 5.380794	4.38E-08 5.646125	1.55E-09 5.801861

TABLE 10. H^1_ε error and convergence rate using C^1 quintic splines.

$N \rightarrow$ $\varepsilon \downarrow$	2^4	$2^5/Rate$	$2^6/Rate$	$2^7/Rate$	$2^8/Rate$	$2^9/Rate$
10^{-4}	3.24E-04	4.15E-05 4.374889	3.74E-06 4.706971	2.69E-07 4.884634	1.52E-08 5.138432	4.78E-10 6.009563
10^{-6}	9.85E-05	1.25E-05 4.383308	1.13E-06 4.711465	8.12E-08 4.886553	5.06E-09 4.960245	2.87E-10 4.986968
10^{-8}	3.10E-05	3.95E-06 4.384522	3.56E-07 4.711951	2.55E-08 4.886756	1.59E-09 4.960318	9.03E-11 4.986991
10^{-10}	9.82E-06	1.25E-06 4.387968	1.12E-07 4.712151	8.07E-09 4.88679	5.03E-10 4.960328	2.85E-11 4.986773
10^{-12}	3.16E-06	3.95E-07 4.420918	3.56E-08 4.713684	2.55E-09 4.886934	1.59E-10 4.960343	9.08E-12 4.976415

with Dirichlet, Neumann and Robin boundary conditions has been examined experimentally on several test problems from the literature and expected convergence rates obtained; cf. [26]. The theoretical analysis of this method and its application to time-dependent problems are topics of future research.

TABLE 11. H_ε^2 error and convergence rate using C^1 quintic splines.

$N \rightarrow$ $\varepsilon \downarrow$	2^4	$2^5/Rate$	$2^6/Rate$	$2^7/Rate$	$2^8/Rate$	$2^9/Rate$
10^{-4}	1.31E-03	2.62E-04 3.421217	3.91E-05 3.723914	4.80E-06 3.89053	4.82E-07 4.104504	3.04E-08 4.805521
10^{-6}	3.97E-04	7.92E-05 3.428643	1.18E-05 3.728049	1.45E-06 3.892329	1.58E-07 3.962173	1.59E-08 3.987589
10^{-8}	1.25E-04	2.49E-05 3.429443	3.71E-06 3.728484	4.55E-07 3.892518	4.96E-08 3.962243	5.00E-09 3.987612
10^{-10}	3.95E-05	7.88E-06 3.429735	1.17E-06 3.728532	1.44E-07 3.892537	1.57E-08 3.96225	1.58E-09 3.987614
10^{-12}	1.25E-05	2.49E-06 3.431881	3.71E-07 3.728577	4.55E-08 3.89254	4.95E-09 3.96225	5.00E-10 3.98761

TABLE 12. $W^{1,\infty}$ error and convergence rate using C^1 quintic splines.

$N \rightarrow$ $\varepsilon \downarrow$	$2^4/Rate$	$2^5/Rate$	$2^6/Rate$	$2^7/Rate$	$2^8/Rate$	$2^9/Rate$
10^{-4}	4.69E-01	8.90E-02 3.536312	1.11E-02 4.078207	5.00E-04 5.748956	1.87E-05 5.869859	6.41E-07 5.865856
10^{-6}	4.52E+00	8.53E-01 3.54788	1.06E-01 4.085582	9.61E-03 4.450854	7.00E-04 4.680516	4.38E-05 4.818104
10^{-8}	4.50E+01	8.49E+00 3.549088	1.05E+00 4.086356	9.56E-02 4.451326	6.96E-03 4.680794	4.35E-04 4.818264
10^{-10}	4.50E+02	8.49E+01 3.54921	1.05E+01 4.086433	9.55E-01 4.451373	6.96E-02 4.680821	4.35E-03 4.81828
10^{-12}	4.50E+03	8.49E+02 3.549222	1.05E+02 4.086441	9.55E+00 4.451378	6.96E-01 4.680824	4.35E-02 4.818282

TABLE 13. Maximum absolute nodal error in first derivative and convergence rate using C^1 cubic splines.

$N \rightarrow$ $\varepsilon \downarrow$	2^4	$2^5/Rate$	$2^6/Rate$	$2^7/Rate$	$2^8/Rate$	$2^9/Rate$
10^{-4}	3.62E+00	8.04E-01 3.202438	1.26E-01 3.635568	1.57E-02 3.859531	1.72E-03 3.951259	1.74E-04 3.984083
10^{-6}	3.51E+01	7.77E+00 3.209053	1.21E+00 3.638776	1.51E-01 3.860791	1.65E-02 3.951698	1.67E-03 3.984226
10^{-8}	3.50E+02	7.74E+01 3.209734	1.21E+01 3.639109	1.50E+00 3.860922	1.65E-01 3.951744	1.67E-02 3.984234
10^{-10}	3.50E+03	7.74E+02 3.209803	1.21E+02 3.639142	1.50E+01 3.860935	1.65E+00 3.951749	1.66E-01 3.984243
10^{-12}	3.50E+04	7.73E+03 3.20981	1.21E+03 3.639145	1.50E+02 3.860934	1.65E+01 3.951703	1.67E+00 3.983826

TABLE 14. Maximum absolute nodal error and convergence rate using C^1 quintic splines.

$N \rightarrow$ $\varepsilon \downarrow$	2^4	$2^5/Rate$	$2^6/Rate$	$2^7/Rate$	$2^8/Rate$	$2^9/Rate$
10^{-4}	4.32E-05	2.18E-06 6.352481	5.40E-08 7.239378	2.19E-10 10.217753	8.54E-13 9.912546	3.54E-14 5.532157
10^{-6}	3.98E-05	2.01E-06 6.360358	4.96E-08 7.242241	7.03E-10 7.896552	7.87E-12 8.027456	7.95E-14 7.9867
10^{-8}	3.95E-05	1.99E-06 6.360891	4.92E-08 7.242247	6.97E-10 7.896141	7.80E-12 8.028306	7.93E-14 7.975899
10^{-10}	3.95E-05	1.99E-06 6.360941	4.91E-08 7.242245	6.97E-10 7.896095	7.79E-12 8.02813	8.03E-14 7.952817
10^{-12}	3.95E-05	1.99E-06 6.360946	4.91E-08 7.242244	6.96E-10 7.896091	7.79E-12 8.028435	7.53E-14 8.06406

Acknowledgments

The authors gratefully acknowledge the research support of the Department of Science and Technology, Government of India, through the National Programme on Differential Equations: Theory, Computation and Applications, DST Project

TABLE 15. Maximum absolute nodal error in first derivative and convergence rate using C^1 quintic splines.

$N \rightarrow$ $\varepsilon \downarrow$	2^4	$2^5/Rate$	$2^6/Rate$	$2^7/Rate$	$2^8/Rate$	$2^9/Rate$
10^{-4}	7.03E-02	3.68E-03 6.278407	9.67E-05 7.122586	4.80E-07 9.841753	1.99E-09 9.799622	6.44E-12 9.969293
10^{-6}	6.70E-01	3.49E-02 6.284881	9.17E-04 7.124722	1.50E-05 7.634613	1.83E-07 7.868111	1.88E-09 7.955033
10^{-8}	6.66E+00	3.47E-01 6.285578	9.12E-03 7.124975	1.49E-04 7.634671	1.82E-06 7.86815	1.88E-08 7.953676
10^{-10}	6.66E+01	3.47E+00 6.285648	9.12E-02 7.125	1.49E-03 7.634677	1.82E-05 7.868138	1.87E-07 7.954558
10^{-12}	6.66E+02	3.47E+01 6.285655	9.12E-01 7.125003	1.49E-02 7.634678	1.82E-04 7.868157	1.87E-06 7.959282

TABLE 16. Maximum absolute nodal error and convergence rate using C^1 cubic splines.

$N \rightarrow$ $\varepsilon \downarrow$	2^4	$2^5/Rate$	$2^6/Rate$	$2^7/Rate$	$2^8/Rate$	$2^9/Rate$
2^{-4}	6.9532e-07	4.3205e-08 5.911506	2.6968e-09 5.430182	1.6848e-10 5.144818	1.0552e-11 4.950745	8.3045e-13 4.418185
2^{-6}	6.9946e-06	4.2832e-07 5.942551	2.6632e-08 5.437766	1.6624e-09 5.146392	1.0387e-10 4.954960	6.4727e-12 4.823938
2^{-8}	1.0523e-04	6.1382e-06 6.045875	3.7677e-07 5.463004	2.3441e-08 5.152457	1.4634e-09 4.956496	9.1434e-11 4.819373
2^{-10}	1.4285e-03	9.8320e-05 5.693963	5.7692e-06 5.551183	3.5467e-07 5.174618	2.2075e-08 4.961917	1.3782e-09 4.820670
2^{-12}	3.0702e-03	6.0390e-04 3.459744	7.9417e-05 3.971395	8.7193e-06 4.098678	9.1945e-07 4.019748	9.1313e-08 4.013947
2^{-14}	3.1365e-03	6.1583e-04 3.463592	8.0763e-05 3.976788	5.5946e-06 4.953110	3.4424e-07 4.982374	2.1430e-08 4.825713
2^{-16}	3.0370e-03	5.9798e-04 3.457586	7.8754e-05 3.968542	8.6525e-06 4.097404	9.1272e-07 4.019125	9.0648e-08 4.013900
2^{-18}	3.0205e-03	5.9504e-04 3.456446	7.8425e-05 3.967075	8.6193e-06 4.096759	9.0939e-07 4.018805	9.0318e-08 4.013876
2^{-20}	3.0122e-03	5.9357e-04 3.455861	7.8262e-05 3.966331	8.6029e-06 4.096435	9.0774e-07 4.018638	9.0154e-08 4.013870
2^{-25}	3.0054e-03	5.9237e-04 3.455371	7.8127e-05 3.965714	8.5893e-06 4.096167	9.0638e-07 4.018510	9.0021e-08 4.013817
2^{-30}	3.0042e-03	5.9215e-04 3.455284	7.8104e-05 3.965604	8.5869e-06 4.096119	9.0614e-07 4.018478	9.0009e-08 4.013603

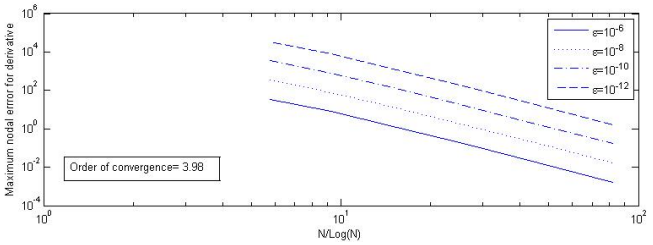

FIGURE 11. Maximum absolute nodal error in first derivative using C^1 cubic splines

No. SERB/F/1279/2011-2012. Support was also received by GF from IIT Bombay while a Distinguished Guest Professor at that institution.

References

[1] Bialecki, B and Fairweather, G. Orthogonal spline collocation methods for partial differential equations. J. Comput. Appl. Math., 128 (2001) 55–82.

[2] Constantinou, P. and Xenophontos, C. Finite element analysis of an exponentially graded mesh for singularly perturbed problems. Comput. Methods Appl. Math., 15(2015) 135–143.

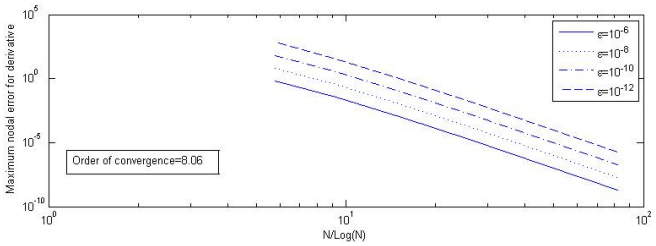

FIGURE 12. Maximum absolute nodal error in first derivative using C^1 quintic splines.

[3] de Boor, C. The method of projections as applied to the numerical solution of two point boundary value using cubic splines. Ph.D. thesis, University of Michigan, Ann Arbor, Michigan, 1966.
[4] de Boor, C. and Swartz, B. Collocation at gaussian points. SIAM J. Numer. Anal., 10(1973) 582–606.
[5] Diaz, J.C., Fairweather, G., and Keast, P. Algorithm 603: Colrow and arceco: Fortran packages for solving certain almost block diagonal linear systems by modified alternate row and column elimination. ACM Trans. Math. Software, 9(1983) 376–380.
[6] Douglas Jr., J and Dupont, T. Collocation methods for parabolic equations in a single space variable. Lecture Notes in Mathematics, Vol. 385, Springer-Verlag, New York-Berlin, 1974.
[7] Douglas Jr., J. and Dupont, T. A finite element collocation method for quasilinear parabolic equations. Math. Comp., 27(1973) 17–28.
[8] Flaherty, J.E. and Mathon, W. Collocation with polynomial and tension splines for singularly-perturbed boundary value problems. SIAM J. Sci. Stat. Comput., 1(1980) 260–289.
[9] Gupta, Y and Kumar, Y. Anthology of spline based numerical techniques for singularly perturbed boundary value problems. Int. J. Pure Appl. Math., 74(2012) 437–453.
[10] Kumar, M and Gupta, Y. Methods for solving singular boundary value problems using splines: a review. J. Appl. Math. Comput., 32(2010) 265–278.
[11] Kadalbajoo, M.K. and Gupta, V. A brief survey on numerical methods for solving singularly perturbed problems. Appl. Math. Comput., 217(2010) 3641–3716.
[12] Kadalbajoo, M.K. and Patidar, K.C. A survey of numerical techniques for solving singularly perturbed ordinary differential equations. Appl. Math. Comput., 130(2002) 457–510.
[13] Kadalbajoo, M.K. and Patidar, K.C. Singularly perturbed problems in partial differential equations: a survey. Appl. Math. Comput., 134(2003) 371–429.
[14] Kadalbajoo, M.K and Aggarwal, V.K. Fitted mesh B-spline collocation method for solving self-adjoint singularly perturbed boundary value problems. Appl. Math. Comput., 161(2005) 973–987.
[15] Linß, T. and Radojev, G. Robust a posteriori error bounds for spline collocation applied to singularly perturbed reaction-diffusion problems. Electron. Trans. Numer. Anal., 45(2016) 342–353.
[16] Linß, T., Radojev, G., and Zarin, H. Approximation of singularly perturbed reaction-diffusion problems by quadratic c^1-splines. Numer. Algorithms, 61(2012) 35–55.
[17] Linß, T. Layer-Adapted Meshes for Reaction-Convection-Diffusion Problems. Lecture Notes in Mathematics 1985, Springer-Verlag, Berlin, 2010.
[18] Miller, J.J.H, O'Riordan, E., and Shishkin, G.I. Fitted numerical methods for singular perturbation problems: error estimates in the maximum norm for linear problems in one and two dimensions. World Scientific, Singapore, 1996.
[19] Mishra, P., Sharma, K.K. Pani, A.K. and Fairweather, G. Orthogonal spline collocation for a class of singularly perturbed reaction diffusion problems in one dimension: A computational study. Technical Report, November (2016), DOI: 10.13140/RG.2.2.15552.94726.
[20] Roos, H.G. Robust numerical methods for singularly perturbed differential equations: A survey covering 2008–2012. ISRN Appl. Math., Art. ID 379547, 2012.
[21] Roos, H.G., Stynes, M. and Tobiska, L. Robust numerical methods for singularly perturbed differential equations: convection-diffusion-reaction and flow problems. Second edition. Springer Series in Computational Mathematics, 24, Springer-Verlag, Berlin, 2008.

[22] Roos, H.G., Teofanov, L. and Uzelac, Z. Graded meshes for higher order fem. J. Comput. Math., 33(2015) 1–16.
[23] Roos, H.G. and Uzelac, Z. Qualocation for a singularly perturbed boundary value problem. J. Comput. Appl. Math., 237(2013) 556–564.
[24] Shishkin, G.I. A difference scheme for a singularly perturbed equation of parabolic type with discontinuous boundary conditions. USSR Computational Mathematics and Mathematical Physics, 28(1998) 32–41.
[25] Shishkin, G.I and Shishkina, L.P. Difference methods for singular perturbation problems, volume 140. CRC Press, Boca Raton, Florida., 2009.
[26] Uzelac, Z. Surla, K. and Pavlović, L. On collocation methods for singular perturbation problems of convection-diffusion type. Novi Sad J. Math., 31(2001) 125–132.
[27] Xenophontos, C. and Oberbroeckling, L. A numerical study on the finite element solution of singularly perturbed systems of reaction–diffusion problems. Appl. Math. Comput., 187(2007) 1351–1367.

Department of Mathematics, South Asian University, Akbar Bhavan, Chanakypuri, New Delhi-110021, India.
E-mail: pmparasar@students.sau.ac.in and kapil.sharma@sau.ac.in

Department of Mathematics, Industrial Mathematics Group, Indian Institute of Technology Bombay, Powai, Mumbai-400076, India.
E-mail: akp@math.iitb.ac.in

Mathematical Reviews, American Mathematical Society, 416 Fourth Street, Ann Arbor, MI 48103, USA.
E-mail: graeme.fairweather@gmail.com